Available online at www.sciencedirect.com
SCIENCE DIRECT
Journal of Fluorine Chemistry 125 (2004) 1791–1799
JOURNAL OF FLUORINE CHEMISTRY
www.elsevier.com/locate/fluor

Dissolution behavior of tetrafluoroethylene-based fluoropolymers for 157-nm resist materials

Takuji Ishikawa[a,*], Tesuhiro Kodani[a], Tomohiro Yoshida[a], Tsukasa Moriya[a], Tsuneo Yamashita[a], Minoru Toriumi[a], Takayuki Araki[a], Hirokazu Aoyama[a], Takuya Hagiwara[b], Takamitsu Furukawa[b], Toshiro Itani[b], Kiyoshi Fujii[b]

[a]*Dakin Industries Ltd., 1-1 Nishi-Hitotsuya, Settsu, Osaka 566-8585, Japan*
[b]*Semiconductor Leading Edge Technologies, Inc. (Selete), 16-1 Onogawa, Tsukuba, Ibaraki 305-8569, Japan*

Abstract

We have synthesized various main-chain fluorinated polymers and studied base-resin properties, such as transparency at 157 nm, solubility in a standard alkaline developer, and lithographic performance. Main-chain-fluorinated polymers were synthesized by copolymerization of tetrafluoroethylene (TFE) with cyclic monomers, especially newly synthesized norbornene derivatives. We studied the correlation between pK_a(OH) and the solubility of the copolymers of TFE and functional (fluoroalkyl alcohol group) norbornenes. Their solubility depends on the pK_a value of the fluoroalkyl alcohol groups.

We studied the impact of the polymerization initiators on base-resin properties. High transparency was obtained by using the fluorocarbon initiator. It was also confirmed that the monocyclic component improves dry-etch resistance and that fluorination at the terminal groups improves alkaline solubility.

In addition, we found that the development characteristics of TFE/norbornene copolymers were significantly improved by the stereoselective (*endo* versus *exo*) partial protection of the hydroxyl groups in the fluoroalkyl alcohol moiety attached to norbornene unit. The polymer protected only in the *exo* position of the norbornene unit in the copolymer had a higher R_{max} and a higher contrast. Positive-working resists based on these fluoropolymers were developed and 55 nm dense lines could be delineated by exposure at 157 nm wavelength with an alternating phase shift mask on a 0.9 NA 157 nm exposure tool.
© 2004 Elsevier B.V. All rights reserved.

Keywords: 157-nm lithography; F_2; Resist; Fluoropolymer; Tetrafluoroethylene; Norbornene; Hexafluoroisopropanol; *Exo*; Polymer reaction; Quartz crystal microbalance

1. Introduction

Photolithography using F_2 laser sources operating at 157 nm is expected to yield the next generation of devices at the sub-65-nm node. One of the key elements required for a successful and timely introduction of 157-nm lithography is the development of a highly transparent resist system that can delineate the fine patterns needed with high aspect ratios. The polymers used in conventional resists show significantly high absorbance at 157 nm, making them difficult to use if the film thickness is greater than 100 nm [1]. Fluorination of polymers has shown its potential for achieving high transparency at 157 nm. Fluoropolymers strongly shift the optical absorption edges to higher energies or shorter wavelengths. This characteristic is one of the great advantages of fluoropolymers for 157-nm lithography.

Fluoropolymers for 157-nm resist base resins have been intensively studied over the past 5 years [2–6]. Two main types of fluoropolymers for 157-nm photoresist have been reported: side-chain-fluorinated polymers and main-chain-fluorinated polymers.

The main-chain-fluorinated polymers have a high fluorine content in the main chain. Fluoro-chemical companies have

* Corresponding author. Tel.: +81 6 6349 5331; fax: +81 6 6349 4751.
E-mail address: takuji.ishikawa@daikin.co.jp (T. Ishikawa).

0022-1139/$ – see front matter © 2004 Elsevier B.V. All rights reserved.
doi:10.1016/j.jfluchem.2004.09.012

been quite active in developing fluoropolymers for use in 157-nm lithography [6–10]. Two types of polymers are widely known: copolymers of tetrafluoroethylene (TFE)/norbornene derivatives and cyclic polymers. These resists are highly transparent; their absorption coefficient is less than 1 μm^{-1} and can approach ca. 0.4 μm^{-1}. Fluorination of the polymer backbone effectively reduces the transparency at 157 nm and strengthens dry-etching durability. Main-chain-fluorinated polymers also have the advantage of high transparency at the wavelength of 157 nm, so they are a practical choice for the single-layer resist process [5].

The other equally important point is solubility of the hydrophobic fluoropolymers in aqueous bases due to the importance of high dissolution rates. One answer is the use of fluoroalchol moiety, especially hexafluoroisopropanol (HFA) group, which has an acidity similar to that of phenolic hydroxyl group. Various new fluoropolymers using HFA as an acidic unit have been reported for 157-nm lithography [2–6]. Unfortunately, the dissolution rate of these polymers is still not high enough.

We have intensively studied the modification of polymers of TFE/norbornene as the main-chain-fluorinated polymers to enhance their dissolution rates [9,10]. In this paper, we report the synthesis of main-chain-fluorinated base-resins using the copolymer of TFE and the HFA group containing norbornene, and the relationship between the dissolution behavior and the pK_a of the HFA group of the norbornene monomer. The dissolution rate depends on the pK_a value of the HFA group, which enhances by increasing the number of fluorine substituents in the molecule. Our investigations show that the dissolution property, transparency and development characteristics can be effectively enhanced by changing the end group of the polymer to a fluoroalkyl group.

Furthermore, we found that the development characteristics of TFE/norbornene copolymers was significantly improved by the stereoselective (*endo* versus *exo*) partial protection of the hydroxyl groups in the HFA moiety attached to norbornene unit. For the *exo*- or *endo*-selective synthesis of partially protected polymers, we used two methods on the basis of the difference of chemical reactivity of functional group in *exo* and *endo* substituent attached to norbornene unit (Fig. 1) [11]. One is copolymerization of TFE and the hydroxyl-protected norbornene and the other is selective introduction of the protective group to *exo* HFA moiety in the parent polymer. We describe an *endo*/*exo* effect on their fundamental properties, such as structure, reactivity and transparency at 157 nm, as well as solubility in a standard alkaline developer.

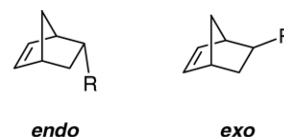

Fig. 1. Norbornenes isomers.

2. Results and discussion

2.1. Synthesis of monomer and polymer

Our approach to the design of 157 nm fluoropolymers is to alternate the copolymers of tetrafluoroethylene and HFA-substituted norbornenes (Fig. 2). Our functional norbornenes differ from those reported by others; the main-chain-fluorinated polymer composed of our functional norbornenes has stronger hydrophilicity. Alkaline solubility of the polymer depends on their acidities, which can be changed by introducing fluorine into the neighborhood of the HFA group. The hydroxyl group in the side chain offers several benefits such as better substrate adhesion during the spin-coating process, wettability, solubility during the development process and so on.

The HFA group containing norbornenes were synthesized by the Diels–Alder reaction of cyclopentadiene and fluorinated vinyl compounds (Fig. 3). In particular, norbornene **4** was obtained in 90% yield with an *exo*-rich adduct through two-step reaction as shown in Fig. 4. The ratio of *endo*/*exo* isomer was 30/70 after distillation. While in general, the Diels–Alder reaction of cyclopentadiene with acrylate derivatives selectively yields an *endo*-rich adduct, it was reported that α-fluoro-acrylate derivatives selectively yields an *exo*-rich adduct [12].

The TFE/functional norbornene polymers are easily synthesized in a solution of TFE and functional norbornene with radical initiators. The resulting copolymers were found to have T_g of 125–135 °C and M_w of 2000–10,000.

2.2. Dissolution rate and pK_a(OH) of functional norbornenes

We studied the relationship between the dissolution behavior of copolymers and pK_a of the HFA group of the norbornene monomer. The dissolution behavior was measured by a quartz crystal microbalance (QCM) method [13]. The developer used was 0.26N tetramethylammonium hydroxide (TMAH) aqueous solution. We also measured the contact angles of water drops on the copolymers. Table 1

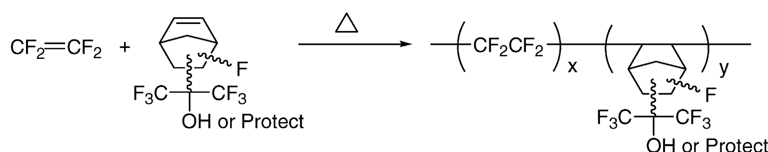

Fig. 2. TFE/functional norbornene copolymer for 157-nm lithography resist.

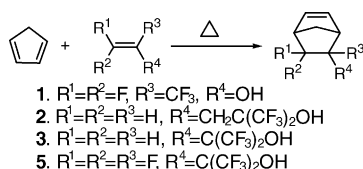

Fig. 3. Synthesis of functional norbornenes.

Table 1
Norbornenes and experimental results

Norbornene	pK_a	Dissolution rates (nm/s)	Contact angle (°)	Polymer F cont. (%)
1	11.5	0	75	54
2	10.5	0	72	53
3	10.2	7	72	53
4	9.0	170	77	55
5	8.3	40	92	60

shows fluorine content and pK_a(OH) of the monomers, dissolution rates and copolymer water contact angles.

This shows that the dissolution rates of copolymers increased with the acidity of the –OH groups. The pK_a(OH) of the monomers increased with fluorine concentration around the –OH groups, so in addition to acidity, water repellency was also increased. When polymer water repellency was too high, the polymer had poor dissolution rate even if it incorporated –OH with high acidity. Thus, control of the fluorine content is important for obtaining a highly soluble copolymer.

2.3. Terminal effects of the TFE/functional norbornene polymers

The synthesized fluoropolymers had almost the same molecular weight, 5000. The terminal effects of the polymers can be clearly recognized at low molecular weight. The effect decreases as the molecular weight of the polymer increases.

2.3.1. Optical characteristics

Fig. 5 shows the polymerization initiators evaluated: A–F. Fig. 6 shows the VUV spectra of the fluoropolymers polymerized by two typical initiators D and F. The absorption coefficients are summarized in Table 2. The initiators can be classified into two groups: initiators C and D, and the other initiators. The former initiator group produces polymers with larger absorption coefficients at 157 nm, and the latter group polymers with lower absorption coefficients. We measured the infrared (IR) spectrum of the polymers prepared using these initiators. The former group shows a carbonyl vibration peak in the IR chart, while the latter does not. The difference in the polymerization mechanisms can explain this effect as shown in Fig. 7. Fig. 7(b) shows the conventional reaction mechanism of the latter initiator group, initiators A, B, E and F. The reaction produces alkyl radicals after the thermal decomposition and decarboxylation. Those radicals can initiate the polymerization or terminate the reaction by radical recombination. The fluoropolymers may have the alkyloxy end-capping terminal in the case of termination. This mechanism does not include the formation of a carbonyl group at the terminals. In the case of the former initiator group, C and D, this intermediate or the carboxyl radical may contribute to the mechanism before decarboxylation (see Fig. 7(a)). For instance, this is true when the initiation fluoropolymer has a carbonyl end-capping, even though this mechanism is a competitive reaction with the conventional reaction channel. This mechanism can well explain the IR experimental results, which shows the existence of a carbonyl group.

Table 2
Initiators and experimental results

Initiator	Terminal size[a] (Å^3)	Absorption coefficient (μm^{-1})	Dry-etching rate relative to KrF resist	Dissolution rate (nm/s)
A	52	0.42	1.7	320
B	135	0.72	1.7	9
C	74	0.80	1.9	480
D	182	0.93	1.7	170
E	153	0.46	1.6	130
F	52	0.39	2.0	860

[a] Terminal size was determined by iso-electron density volumes quantum-chemically calculated on the typical terminal structure.

Molecular sizes of end-capping groups are also listed in Table 2. It shows that the smaller terminals reduce the absorption coefficients. This is a dilution effect, which shows up more notably with smaller terminals.

2.3.2. Dry-etching durability

The carbonyl group also affects the dry-etch durability. We measured the dry-etch rate relative to KrF resist under the contact hole etching condition; the results are summarized in Table 2. The monocyclic functional group improves the dry-etch resistance (compare initiator C to initiator D). The fluoroalkyl terminals of initiator F show weaker durability. Fluorination might increase the dry-etching rate because volatile fluorides are generated during the etch process.

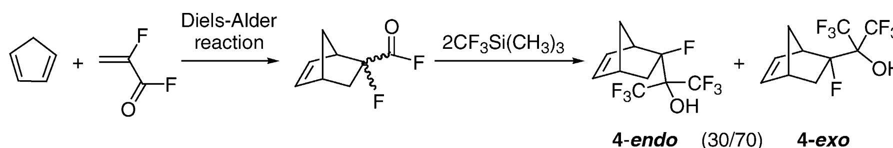

Fig. 4. Synthesis of functional norbornene **4**.

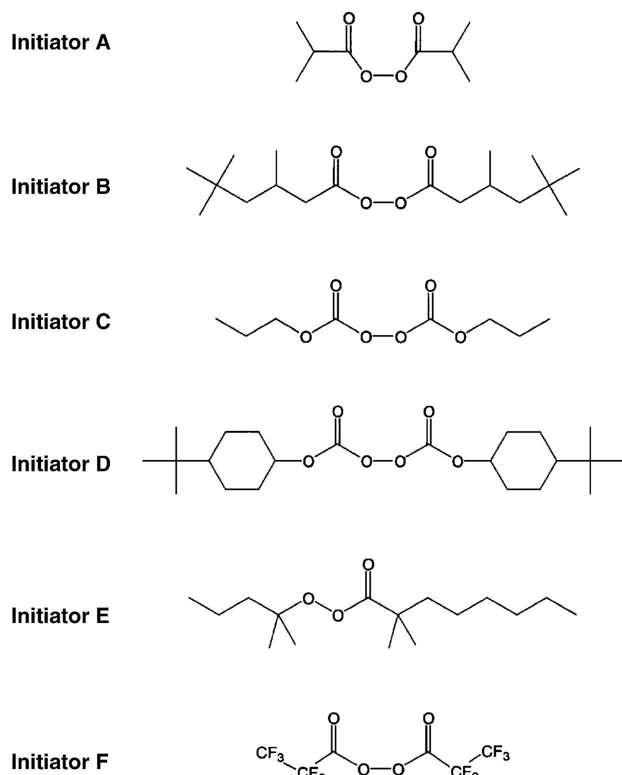

Fig. 5. Molecular structures of the evaluated initiators.

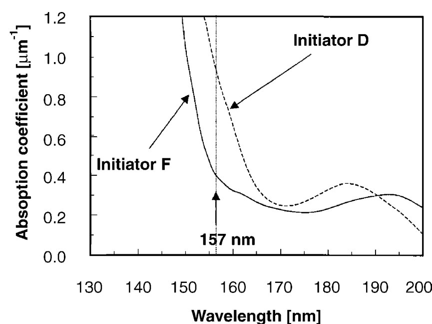

Fig. 6. VUV spectra of the tetrafluoroethylene/functionalized norbornene polymers obtained using initiators D and F.

2.3.3. Dissolution characteristics

Unprotected fluoropolymers should show larger dissolution rates without swelling in the standard developer (a 2.38 wt.% tetramethylammonium hydroxide aqueous solution). The dissolution rates are summarized in Table 2 and Fig. 8. All evaluated fluoropolymers dissolved well without swelling in the standard developer. The swelling was depressed by the molecular structure of moderately hydrophilic norbornene derivatives. The smaller terminals offer larger dissolution rates. The larger terminals may decrease the dissolution rate due to their larger hydrophobicity.

Note that the fluoroalkyl terminal shows the largest dissolution rate in Table 2. This is considered to be the result of the increase in acidity induced by the initiator. Fluorine attracts the electrons in the neighborhood. This reduces the electron density at the acidic functional group and facilitates the dissociation of the proton yielding an acidic functional group with higher acidity. This fluorination effect was evaluated theoretically by quantum chemistry. We calculated the pK_a of the model compounds shown in Fig. 9. The semi-empirical quantum-chemical calculation, PM1, shows that the pK_a of fluoropolymer decreases from 6.0 (a) to 5.0 (b) when the hydrocarbon terminal is replaced by the fluorocarbon terminal. The increase in acidity by the fluorination of the polymer terminals is another advantage, in addition to the higher transparency at 157 nm.

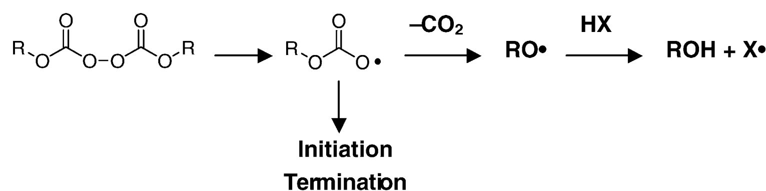

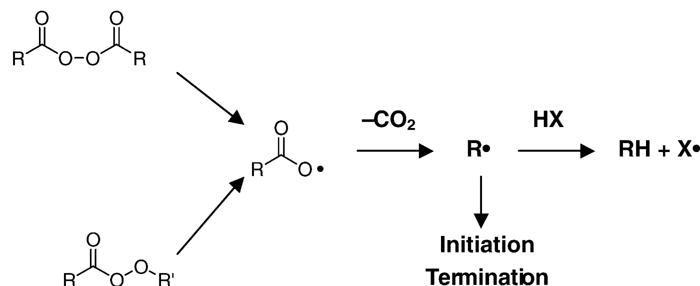

Fig. 7. Polymerization kinetics of (a) initiators C and D and (b) initiators A, B, E and F.

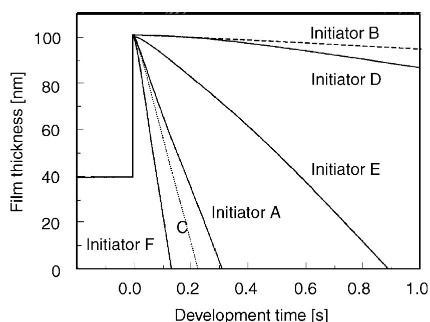

Fig. 8. Dissolution behavior of fluoropolymers polymerized by initiators A–F.

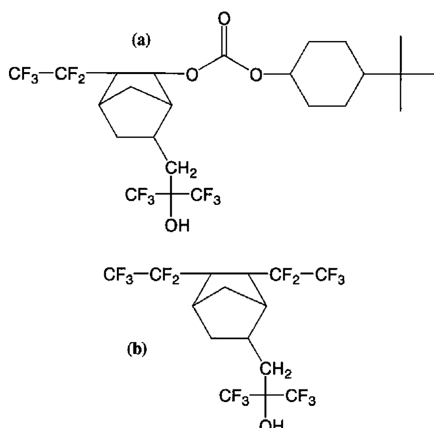

Fig. 9. Model compounds to evaluate the pK_a change by terminal effects.

2.4. Exo/endo selectivity and reactivity of the protective group in the polymer

2.4.1. Partial protection: exo/endo selectivity

The HFA group is easily protected by conventional methods. Protection alters the sensitivity and imaging ability of the resist materials. Partial protection of the hydroxyl groups derived from TFE/functional norbornene polymers was carried out by two methods (Fig. 10): copolymerization (Method A) or polymer reaction (Method B). The partial protection by copolymerization was conducted by copolymerizing TFE with a mixture of protected and unprotected monomer (Method A). The monomer was protected by the ethoxymethyl group. The partial protection by polymer reaction was carried out by reacting the unprotected polymer with ethoxymethyl chloride in the presence of amine (Method B). Both polymers showed excellent 157-nm transparency (absorption coefficient of 0.33 and 0.34, respectively) as shown in Fig. 11.

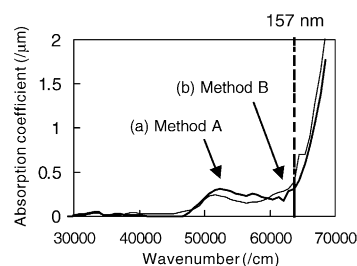

Fig. 11. VUV spectra for the protected TFE/functional norbornene polymer: (a) polymer A (partial protection by copolymerization (Method A)) and (b) polymer B (partial protection by polymer reaction (Method B)).

Fig. 12 shows the ^{19}F NMR spectra of partially protected polymers. Peaks I (57 ppm) and II (62 ppm) were assigned to the CF_3 of the protected HFA group derived from *endo* and *exo* position, respectively. Peak III (66 ppm) was identified with CF_3 of the unprotected HFA group. There is a difference in the ^{19}F NMR spectra between methods A and B. The polymer A (partial protection by copolymerization (Method A)) exhibited peaks I, II and III because it was polymerized using the mixture of protected *endo* and *exo* isomers. The polymer B (partial protection by polymer reaction (Method B)) showed peaks II and III, but peak I was not observed. Therefore, only the HFA group in the *exo* position in the polymer was protected in the polymer reaction.

2.4.2. Reactivity of the protective group in the polymer

Next, the partially protected polymers shown in Fig. 12 were deprotected in mild condition (aq. HCl in MeOH for 3 h) to investigate the reactivity of the protective group in the

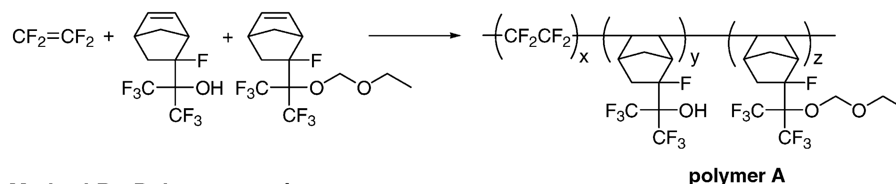

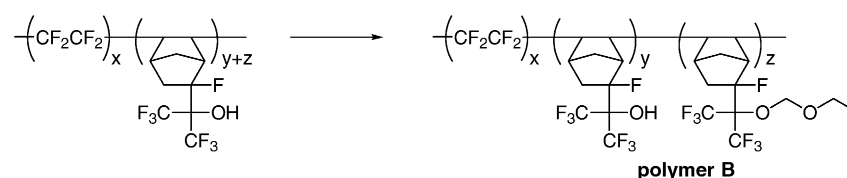

Fig. 10. Partial protection of hydroxyl groups derived from TFE/functional norbornene polymers.

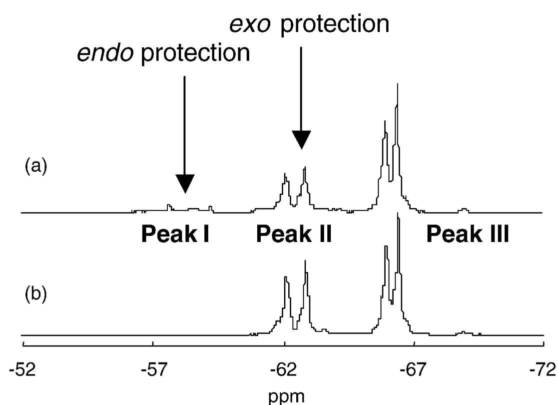

Fig. 12. ^{19}F NMR spectra of the protected TFE/functional norbornene polymer in aceton-d_6: (a) polymer A (partial protection by copolymerization) and (b) polymer B (partial protection by polymer reaction).

polymer. Fig. 13 shows the ^{19}F NMR spectra of the resulting polymers. In deprotection of the polymer A, protective groups in the *exo* position changed to hydroxyl groups but in the *endo* position remained. On the other hand, all protective groups changed to hydroxyl groups in the deprotection of the polymer B. It is considered that the reactivity of deprotection at the *endo* position is much lower than that at the *exo* position, because the *endo* position exhibits larger steric hindrance at the reaction site.

The dissolution behavior of spin-coated films in 0.26N TMAH was investigated using QCM to compare the behavior of two deprotected polymers as shown in Fig. 14. The polymer B had a higher dissolution rate (291 nm/s versus 233 nm/s), although the deprotection condition and the molecular weight of the polymers evaluated in Fig. 14 were almost the same.

2.4.3. Development characteristic

The development characteristic of a resist based on the polymers A and B was also investigated (see Fig. 15). A resist formulation was made by dissolving TFE/functional norbornene polymer (the polymer A or B) and TPSTf in 2-heptanone. Initially, the spin-coated films were exposed to F_2 laser. Then, the dissolution behavior of the exposed films in alkaline developer was investigated using QCM. The exposure was changed from 0.5 to 100 mJ/cm^2. The dissolution rate of the exposed polymer was measured using QCM. The polymer B had a higher dissolution rate ($R_{\max}$) and a higher contrast.

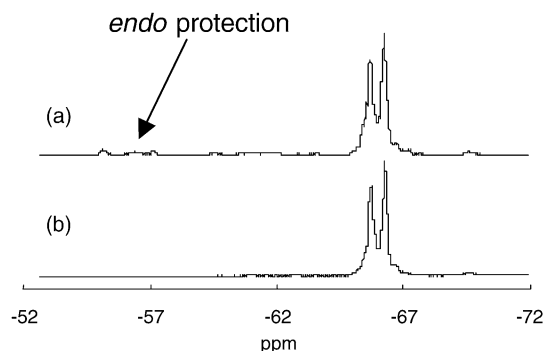

Fig. 13. ^{19}F NMR spectra of the deprotected TFE/functional norbornene polymer in acetone-d_6: (a) deprotection of polymer A and (b) deprotection of polymer B.

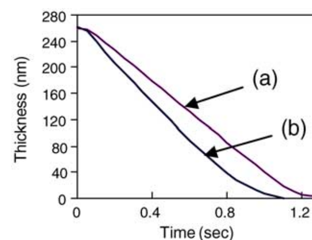

Fig. 14. Dissolution behavior of the deprotected TFE/functional norbornene polymer in 0.26N TMAH: (a) deprotection of polymer A and (b) deprotection of polymer B.

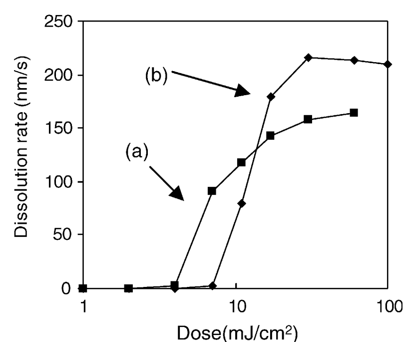

Fig. 15. Dissolution contrast of the TFE/functional norbornene polymer with TPSTf: (a) polymer A and (b) polymer B.

2.4.4. Lithograph performance

A preliminary formulation was made by dissolving a platform polymer B and TPSTf in 2-heptanone. The contrast curve for a resist based on polymer B is shown in Fig. 16. The onset of de-protection is observed at about 3.7 mJ/cm^2. It did not exhibit any negative-tone behavior up to 100 mJ/cm^2. Fig. 17 shows typical imaging result using an Exitech

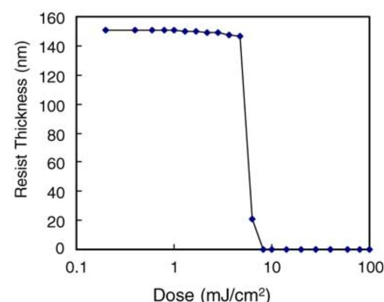

Fig. 16. Sensitivity curve of a resist based on polymer B.

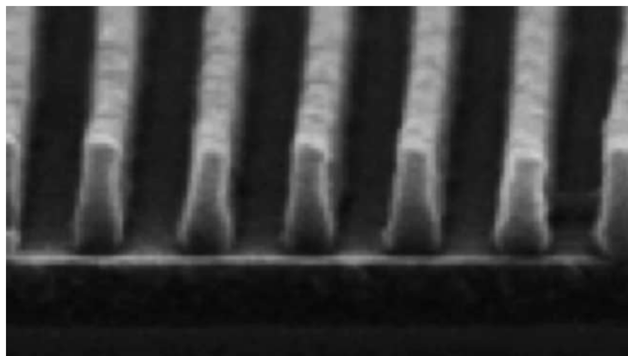

Fig. 17. 157-nm exposure of a resist based on polymer B. Conditions: 150 nm thickness, Exitech Microstepper, NA = 0.90, σ = 0.3, alternating phase-shift mask, PB 110 °C, 90 s, PEB 110 °C, 90 s, DEV 60 s.

mini-stepper (0.90 NA) by using an alternating phase-shift mask. We achieved 55 nm 1:1 line and space patterns in a 150-nm thick film using the resist formulation based on polymer B.

3. Conclusion

We synthesized various main-chain fluorinated polymers by co- or terpolymerization of tetrafluoroethylene (TFE) with cyclic monomers, with particular emphasis on newly synthesized norbornene derivatives. We studied the correlation between pK_a(OH) and the solubility of the copolymers of TFE and functional (fluoroalkyl alcohol group) norbornenes. The pK_a(OH) of fluoroalkyl alcohol groups was lower with higher fluorine contents, and the solubility of the copolymers tended to be higher with lower pK_a(OH) of the fluoroalkyl alcohol groups. We found norbornene derivative **4** which has compatible acidity and water repellence. We also obtained a TFE/functional norbornene that has high dissolution rate in the standard developer.

We investigated the impact of polymerization initiator on the polymerization of TFE and functionalized norbornene. The carbonyl group incorporated into the polymer chain deteriorates the optical transparency at 157 nm and the dry-etch resistance. Some initiators yield a high transparency of 0.39–0.46 μm^{-1}, a reasonable dry-etch resistance of only 1.6–1.7 times larger than that of KrF resists, and larger dissolution rates. Fluorocarbon initiators in particular resulted in dissolution rates of up to 800 nm/s in the standard developer.

We demonstrated that the development characteristics of a TFE/HFA group containing norbornenes could be improved by increasing the reactivity of the protective group in the copolymer. We showed that the protective group was introduced only in the *exo* position of the norbornene unit in the copolymer when partial protection was carried out by the polymer reaction (Method B). The polymer protected by the polymer reaction (polymer B) had a higher R_{max} and a higher contrast due to the higher reactivity of the HFA group in the *exo* position. Preliminary trials showed that resists based on our polymer can provide excellent lithographic performance for dense 55-nm 1:1 line and space patterns in a 150-nm thick film.

4. Experimental

4.1. Materials

All materials were obtained from commercial suppliers and used without further purification, unless otherwise noted. Functional norbornene **4** was prepared by the cycloaddition of cyclopentadiene and α-fluoro-acryl fluoride as described in the literature [12].

4.1.1. Synthesis of 1,1,1,3,3,3-hexafluoro-2-(2-fluoro-bicyclo[2.2.1]hept-5-en-2-yl)-propan-2-ol (4)

2-Fluoro-bicyclo[2.2.1]hept-5-ene-2-carbonyl fluoride (126 g, 0.80 mol) was added to a suspension of dry KF (51 g, 0.88 mol) and dry CsF (12 g, 0.08 mol) in anhydrous THF (1.0 l) under nitrogen. Trifluoromethyltrimethylsilane (250 g, 1.76 mol) was slowly added dropwise into the mixture under nitrogen at 10 °C. The reaction mixture was stirred at room temperature overnight. After the reaction was completed, 500 ml of 1.0N HCl was added to the mixture and extracted with 500 ml of diethyl ether. The combined ether extracts were washed with 1.0N HCl, water and brine. The ether solution was dried over $MgSO_4$, evaporated and distilled at 60 °C at 5 mmHg to yield 198 g (90%) of functional norbornene (**2**) as a colorless oil.

4.1.2. Radical polymerization

The typical polymerization procedure is as follows. A 100-ml stainless steel pressure vessel was charged with a solution of monomers, solvents, and initiator. The vessel was closed, purged with nitrogen, cooled, evacuated, and charged with TFE monomer. Radical copolymerization was carried out at 40 °C and maintained for 18–24 h. The reaction mixture was poured into hexane, and the precipitates washed by hexane. The resulting polymer powder was dried in vacuum.

4.2. Characterization

The polymer structures and compositions were determined from the NMR spectra. Namely, ^{1}H and ^{19}F NMR spectra were obtained at room temperature in acetone-d_6 or $CDCl_3$ using a Brucker AC-300P FT-NMR spectrometer. The polymer structures were also confirmed by the FT-IR spectra recorded by a Perkin Elmer 1760X FT-IR spectrometer.

UV measurements at 157 nm were performed using a VUV-VASE spectroscopic ellipsometer (J.A. Woollam Co., Inc.). The sample films were cast on a CaF_2 plate from solutions and baked at 110 °C for 60 s prior to measure-

ments. Film thickness was measured by using an interferometer. All absorbance data reported are in the base of 10.

The dissolution behavior (i.e. the dissolution kinetics of the polymer film) during the development of the film was studied by a quartz crystal microbalance (QCM, Maxtek Model TM-400) in a fashion similar to a reported procedure [14]. The QCM instrumentation in combination with a compensated phase-locked oscillator circuit can measure the changes of film mass and motional resistance simultaneously during development. The developer used was a 0.262N tetramethylammonium hydroxide (TMAH) aqueous solution (PD-523) supplied from Japan Synthetic Rubber Co., Ltd.

Water repellency of the polymer was estimated from the contact angle of a water drop on the sample film. The sample was dissolved in acetone and cast onto a glass substrate, and dried at room temperature for over 12 h. A 0.3-μl water drop was placed on the film and its contact angle was measured.

4.3. Lithography

Polymers were dissolved in casting solvent, to which was added a photoacid generator (PAG). Triphenylsulfonium triflate (TPSTf), obtained from Midori Kagaku Co. Ltd., which was used in this study as a standard onium PAG. The resist solution was filtered through a 0.2-μm membrane filter. Resist-formulation solvents used in this study included 2-heptanone. The resist solution was spin-coated onto silicon wafers treated with organic antireflective coatings. Pre-application baking and post-exposure baking were carried out in the temperature range of 110 °C for 60–90 s, and the resist was developed. Contrast measurements were conducted by open-frame exposures. From these measurements, the clearing dose for the resist was determined. Cross-sectional scanning electron micrographs were recorded with a Hitachi S-5000 scanning electron microscope.

Acknowledgments

The authors thank Dr. Yuzo Komatsu and Takuji Kume of the chemical division for synthesizing the monomers.

References

[1] R.R. Kunz, T.M. Bloomstein, D.E. Hardy, R.B. Goodman, D.K. Downs, J.E. Curtin, Proc. SPIE 3678 (1999) 13–23;
T.H. Fedynyshyn, R.R. Kunz, S.O. Doran, R.B. Goodman, M.L. Lind, J.E. Curtin, Proc. SPIE 3999 (2000) 335–346;
T.H. Fedynyshyn, R.R. Kunz, R.F. Sinta, M. Sworin, W.A. Mowers, R.B. Goodman, S.P. Doran, Proc. SPIE 4345 (2001) 296–307;
T.H. Fedynyshyn, W.A. Mowers, R.R. Kunz, R.F. Sinta, M. Sworin, R.B. Goodman, Proc. SPIE 4690 (2002) 29–40.

[2] H. Ito, W.D. Hinsberg, L.F. Rhodes, C. Chang, Proc. SPIE 5039 (2003) 70–79;
H. Ito, H.D. Truong, M. Okazaki, D.C. Miller, N. Fender, G. Breyta, P.J. Brock, G.M. Wallraff, C.E. Larson, R.D. Allen, Proc. SPIE 4690 (2002) 18–28;
H. Ito, G.M. Wallraff, P. Brock, N. Fender, W.D. Hinsberg, H. Truong, G. Breyta, D.C. Miller, M.H. Sherwood, R.D. Allen, Proc. SPIE 4345 (2001) 273–284.

[3] V.R. Vohra, X. Liu, K. Douki, C.K. Ober, Proc. SPIE 5039 (2003) 539–547;
V.R. Vohra, K. Douki, Y. Kwark, X. Liu, C.K. Ober, Y.C. Bae, Proc. SPIE 4690 (2002) 84–93;
Y.C. Bae, K. Douki, T. Yu, J. Dai, D. Schmaljohann, S.H. Kang, K.H. Kim, H. Koerner, W. Conley, D. Miller, R. Balasubramania, S. Holl, C.K. Ober, J. Photopolym. Sci. Technol. 14 (2001) 613–620;
D. Schmaljohann, Y.C. Bae, G.L. Weibel, A.H. Hamad, C.K. Ober, Proc. SPIE 3999 (2000) 330–334.

[4] Y. Uetani, K. Hashimoto, Y. Miya, I. Yoshida, M. Takigawa, R. Hanawa, Proc. SPIE 4345 (2001) 379.

[5] T. Chiba, R.J. Hung, S. Yamada, B. Trinque, M. Yamachika, C. Brodsky, K. Patterson, A. Heyden, A. Anthony, S.-H. Jamison, M. Lin, J. Somervell, W. Byers, C.G. Conley, J. Willson, Photopolym. Sci. Technol. 13 (2000) 657–664;
R.J. Hung, H.V. Tran, B.C. Trinque, T. Chiba, S. Yamada, D.P. Sanders, E.F. Connor, R.H. Grubbs, J. Klopp, J.M.J. Frechet, B.H. Thomas, G.J. Shafer, D.D. DesMarteau, W. Conley, C.G. Willson, Proc. SPIE 4345 (2001) 385–395;
B.C. Trinque, B.P. Osborn, C.R. Chambers, Y. Hsieh, S. Corry, T. Chiba, R.J. Hung, H.V. Tran, P. Zimmerman, D. Miller, W. Conley, C.G. Willson, Proc. SPIE 4690 (2002) 58–68;
R.R. Dammel, R. Sakamuri, S. Lee, M.D. Rahman, T. Kudo, A. Romano, L. Rhodes, J. Lipian, C. Hacker, D.A. Barnes, Proc. SPIE 4690 (2002) 101–111;
L. Sharif, D. DesMarteau, L. Ford, G.J. Shafer, B. Thomas, W. Conley, P. Zimmerman, D. Miller, G.S. Lee, C.R. Chambers, B.C. Trinque, T. Chiba, B.P. Osborn, C.G. Willson, Proc. SPIE 5039 (2003) 33–42.

[6] M.K. Crawford, A.E. Feiring, J. Feldman, R.H. French, M. Periyasamy, F.L. Schadt III., R.J. Smalley, F.C. Zumsteg, R.R. Kunz, V. Rao, L. Liao, S.M. Holl, Proc. SPIE 3999 (2000) 357–364;
M.K. Crawford, A.E. Feiring, J. Feldman, R.H. French, V.A. Petrov, F.L. Schadt III., R.J. Smalley, F.C. Zumsteg, Proc. SPIE 4345 (2001) 428–438;
M.K. Crawford, W.B. Farnham, A.E. Feiring, J. Feldman, K.W. Leffew, V.A. Petrov, W. Qiu, F.L. Schadt III., H.V. Tran, R.C. Wheland, F.C. Zumsteg, Proc. SPIE 5039 (2003) 80–92.

[7] T. Yamazaki, T. Furukawa, T. Itani, T. Ishikawa, M. Koh, T. Araki, M. Toriumi, T. Kodani, H. Aoyama, T. Yamashita, Proc. SPIE 5039 (2003) 103–112;
S. Ishikawa, S. Irie, T. Itani, Y. Kawaguchi, O. Yokokoji, S. Komada, Proc. SPIE 5039 (2003) 580–588;
M. Toriumi, N. Shida, H. Watanabe, T. Yamazaki, S. Ishikawa, T. Itani, Proc. SPIE 4690 (2002) 191–199;
N. Shida, H. Watanabe, T. Yamazaki, S. Ishikawa, M. Toriumi, T. Itani, Proc. SPIE 4690 (2002) 497–503;
M. Toriumi, S. Ishikawa, S. Miyoshi, T. Naito, T. Yamazaki, M. Watanabe, T. Itani, Proc. SPIE 4345 (2001) 371–378.

[8] Y. Kawaguchi, J. Irisawa, S. Kodama, S. Okada, Y. Takebe, I. Kaneko, O. Yokokoji, S. Ishikawa, S. Irie, T. Hagiwara, T. Itani, Proc. SPIE 5039 (2003) 43–52;
S. Kodama, I. Kaneko, Y. Takebe, S. Okada, Y. Kawaguchi, N. Shida, S. Ishikawa, M. Toriumi, T. Itani, Proc. SPIE 4690 (2002) 76–83.

[9] M. Koh, T. Ishikawa, T. Araki, H. Aoyama, T. Yamashita, T. Yamazaki, H. Watanabe, M. Toriumi, T. Itani, Proc. SPIE 5039 (2003) 589–599.

[10] M. Toriumi, M. Koh, T. Ishikawa, T. Kodani, T. Araki, H. Aoyama, T. Yamashita, T. Yamazaki, T. Furukawa, T. Itani, Proc. SPIE 5039 (2003) 53–60.
[11] A.E. Feiring, M.K. Crawford, W.B. Farnham, J. Feldman, R.H. French, K.W. Leffew, V.A. Petrov, F.L. Schadt III., R.C. Wheland, F.C. Zumsteg, J. Fluorine Chem. 122 (2003) 11–16, Polymerization of TFE and norbornenes:.
[12] M. Essers, C. M-Lichtenfeld, G. Haufe, J. Org. Chem. 67 (2002) 4715–4721;
H. Ito, A. Saito, A. Kakuuchi, T. Taguchi, Tetrahedron 55 (1999) 12741–12750.
[13] H. Ito, N. Seehof, R. Sato, T. Nakayama, M. Ueda, ACS Symp. Ser. 706 (1998) 208–223.
[14] M. Toriumi, T. Ohfuji, M. Endo, H. Morimoto, J. Photopolym. Sci. Technol. 12 (1999) 545–552;
M. Toriumi, S. Ishikawa, T. Itani, Forefront of Lithographic Materials Research, Society of Plastic Engineers, Society of Plastic Engineers, Mid Hudson Section., 2001, pp. 271–281;
M. Toriumi, T. Itani, J. Yamashita, T. Sekine, K. Nakatani, Proc. SPIE 4690 (2002) 904–910, and references therein.